JOURNAL OF MATERIALS SCIENCE **40** (2005) 5475–5482

Superplasticity and associated activation energy in Ti-3Al-8V-6Cr-4Mo-4Zr Alloy

A. SALAM*, C. HAMMOND
Institute for Materials Research, University of Leeds, Leeds, U.K.
E-mail: materials@leeds.sc.uk

The high temperature deformation characteristics of a commercial β-titanium alloy Ti-3Al-8V-6Cr-4Mo-4Zr have been studied in the temperature range 830–925°C. The alloy exhibited superplasticity in a narrow temperature and strain rate range i.e. 850–865°C and 5×10^{-5}–3×10^{-3} s^{-1} respectively, with a maximum elongation of 634% at 855°C. The superplastic behaviour in the alloy is considered to arise as a result of subgrain formation at the higher strain rates (region III) which enhances diffusional creep at lower strain rates (region II). The activation energy values for regions II and III were found to be close to the lower of the two activation energy values (129.2 KJ/mole) proposed to describe self diffusion in β-phase suggesting that the rate controlling mechanism during high temperature deformation of the alloy was that for lattice diffusion.

1. Introduction

There has been limited work reported on superplasticity in β-titanium alloys as compared to $\alpha + \beta$ titanium alloys. Griffiths and Hammond [1 ,2] reported superplasticity in Ti – 8 Mn, Ti – 15 Mo and Ti-13 Cr-11 V – 3Al in the temperature range 770–900°C. It was suggested that the deformation in these alloys occurred by a process of Herring- Nabarro creep in which the subgrain size represents the characteristic diffusion path. It was also suggested that diffusional creep mechanisms contribute to the deformation of β-titanium alloys to a greater extent as compared to other materials at similar homologous temperatures because of the anomalous diffusional properties of the β-phase. Hamilton et al. [3] also reported superplasticity in three β-titanium alloys, Ti-10V-2Fe-3Al, Ti-15 V-3 Cr-3Sn – 3Al and Ti-8Mo-8V-2Fe-3Al at 815°C. It was concluded that superplasticity in these alloys is attributable to high diffusivity of the β-phase and subgrain formation is not necessary for superplasticity in β-titanium alloys. However, Morgan and Hammond [4] showed that superplasticity in β-titanium alloys arises both as a result of development of subgrains and because of the anomalous diffusion rates characteristics of β- titanium. This theory was based on their investigation into the high temperature deformation properties of three metastable β-titanium alloys, Ti-11Mo-6Zr-4Sn-0.035Fe, Ti-10V-2Fe-3Al and Ti-3Al-8V-6Cr-4Zr-4Mo. The development of subgrain network was brought about as a result of the deformation.

The aim of the present work was to investigate further the superplastic behaviour of the Ti-3Al-8V-6Cr-4Mo-4Zr alloy to determine the microstructural conditions and the strain rate cycling method which support the maximum elongations obtainable. Some of this work was partially included in a previous study of the same authors [5]. The present work was also aimed at the derivation of activation energy data from the flow stress-strain rate behaviour of the alloy to find the rate controlling mechanism during high temperature deformation.

2. Experimental techniques

The tensile specimens were machined from the bar material and tested in an Instron universal tensile testing machine with a Maye's three zone furnace. A Windsor WHME three zone controller was used to control the test temperature within ±2°C. Temperature was also monitored by the use of thermocouple probes inserted into the specimen grips. Also, argon was passed through the furnace continuously during the test to provide an inert atmosphere. The method of crosshead speed cycling was used for testing the specimens. Prior to each test, carried out under both increasing and decreasing strain rate conditions, specimens were initially strained 10–25% at a high strain rate (approx. 5×10^{-3} s^{-1}) to generate a subgrain microstructure. The specimens were subjected to repeated strain rate cycling i.e. at increasing crosshead speeds in the strain rate range 5×10^{-5}–3×10^{-3} s^{-1}, then decreasing crosshead speeds (1 cycle) and repeated (2nd, 3rd etc. cycles), to see the effect of increasing strain on flow stress—strain rate behaviour and to determine the elongations to fracture. A computer program using Fortran77 language along with a graphics package 'Ghost 80' was used to calculate flow stress (σ), strain rates (ε') and

Present address. Institute of chemical Engineering & Technology, University of the Punjab, Lahore, Pakistan.
0022–2461
DOI: 10.1007/s10853-005-2001-0

strain rate sensitivity (m) values for each cycle and to express the experimental data as ln σ vs. lnε and m vs. ln ε' plots. After the tests, the specimens were sectioned longitudinally both over the grip and gauge length sections in order to compare undeformed and deformed microstructures. The specimens for light and high resolution scanning electron microscopy were prepared in the usual way.

3. Results and discussion

Flow stress-strain rate and strain rate sensitivity—strain rate data obtained from cross-head speed cycling tests at all test temperatures (except 855°C) are presented together, for first increasing strain rate cycles in Fig. 1 and for second increasing strain rate cycles in Fig. 2. It may be seen that flow stress–strain rate data are broadly similar i.e. they are strain-independent, with (a) 830 and 850°C curves and (b) 900 and 925°C curves being close together.

Strain rate sensitivity (m) values obtained from ln σ - lnε data are also shown in Figs 1 and 2 as m vs. ln ε' plots. It is obvious from these figures that there is very little change in m-values with increase in temperature at all strain rates. Also, comparison of Figs 1 and 2 show that m-values are higher during up cycles which were preceded by a 10–20% strain at a high strain rate.

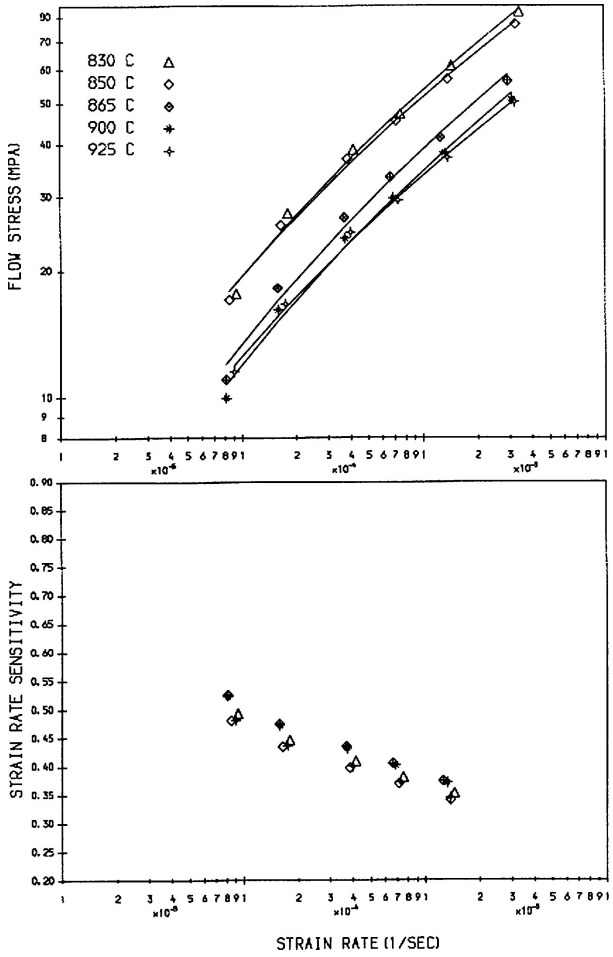

Figure 1 n σ vs. n $\dot{\varepsilon}$ and m vs. n $\dot{\varepsilon}$ plots for Ti-3A1–8V-6Cr-4Mo-4Zr alloy. For each test, only the incresing strain rate part of first cycle is plotted.

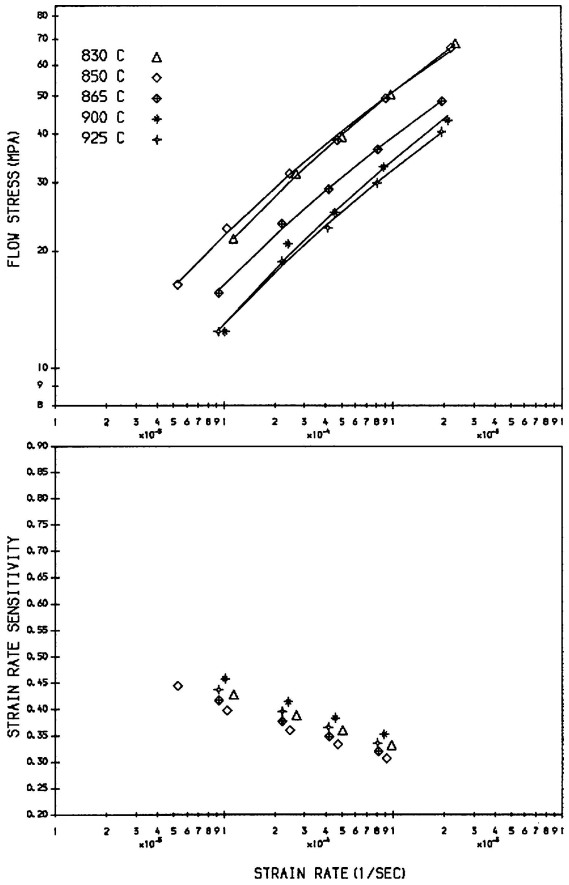

Figure 2 n σ vs. n $\dot{\varepsilon}$ and m vs. n $\dot{\varepsilon}$ plots for Ti-3A1–8V-6Cr-4Mo-4Zr alloy. For each test, only the incresing strain rate part of second cycle is plotted.

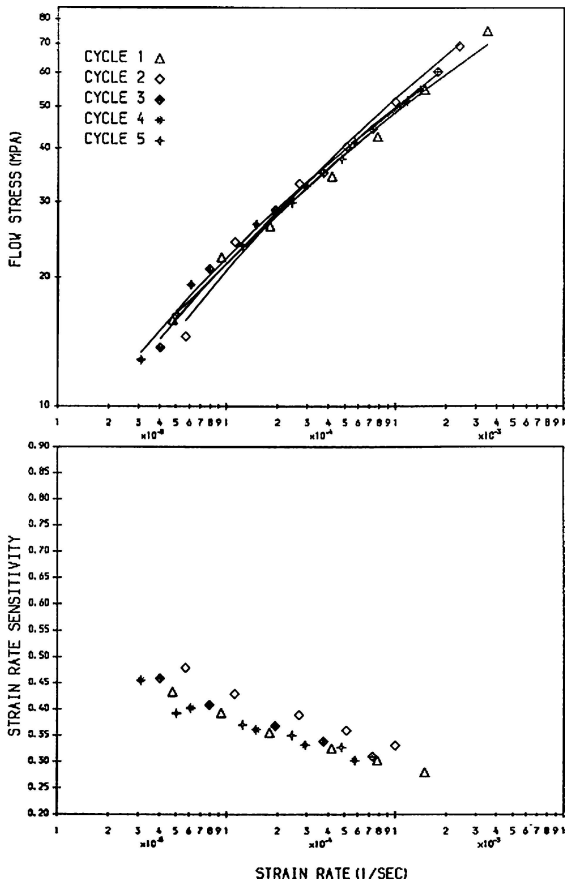

Figure 3 n σ vs. n $\dot{\varepsilon}$ and m vs. n $\dot{\varepsilon}$ plots for Ti-3A1–8V-6Cr-4Mo-4Zr alloy at 855°C. For each test, only the incresing strain rate part of first cycle is plotted.

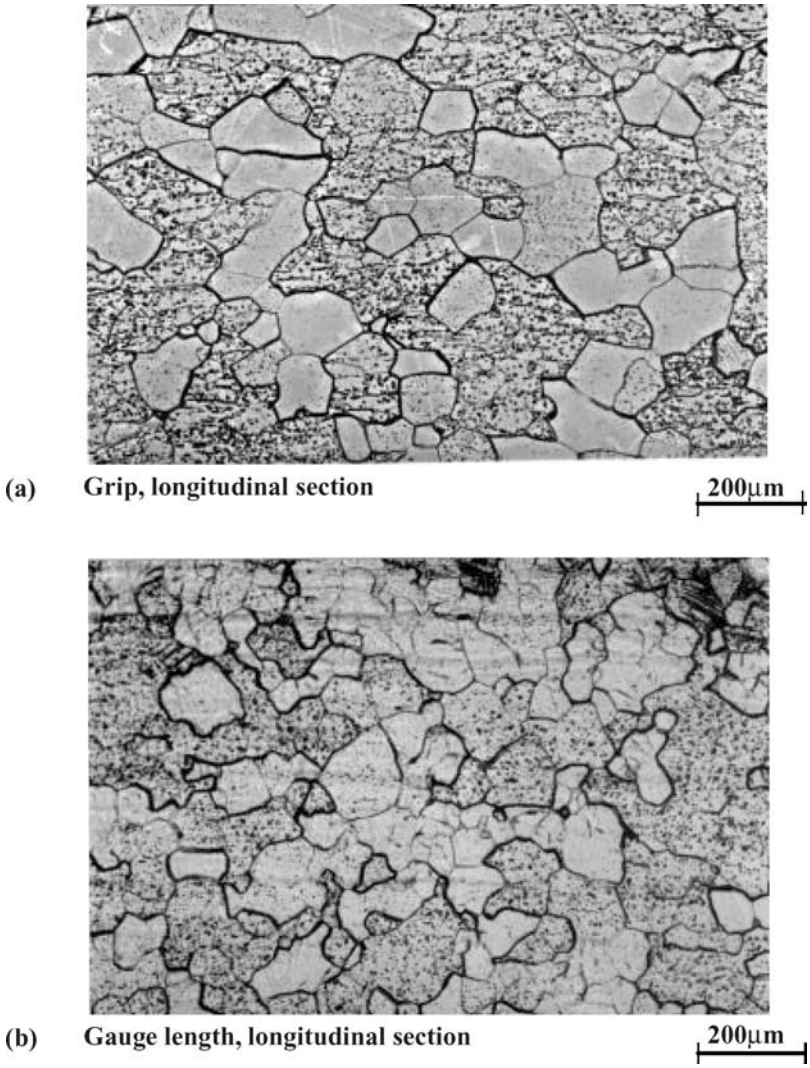

Figure 4 Post test microstructure of Ti-3Al–8V-6Cr-4Mo-4Zr specimen deformed at 855°C, corresponding to a true strain of 1.99.

Maximum m-values are observed at lower strain–rates (0.45–0.52) and they decrease with increasing strain rate.

Elongation to fracture data of specimens are shown in Table I at different temperatures. The elongations first increase with increase in temperature, reaching a maximum of 634% at 855°C and then decrease to 230% at 925°C. At 850 and 855°C the specimens were not deformed to fracture indicating that even higher neck free elongations could be achieved if the tests had been continued. Therefore, 855°C seem to be the optimum temperature at which highest neck free elongation could be achieved in this alloy. Fig. 3 shows ln σ ln ε' and m- ln ε' data up to maximum of five increasing strain rate cycles at 855°C, the temperature at which the highest elongation (634%) was achieved. The figure clearly shows that ln σ - ln ε' data are strain independent at almost all strain rates. At intermediate strain rates, flow stresses are independent of strain whereas at low strain rates there is a small increase in flow stresses during subsequent cycles. Table I also shows that the maximum m-values are maintained close to 0.5 and are almost unaffected by the change in temperature. It may also be seen that the highest elongations obtained at 855 and 850°C do not correspond to the highest m-values (≈0.54 at 900°C). These data show the importance of conducting high temperature deformation tests to maximum elongation in order to study superplastic behaviour of β-titanium alloys, because strain rate sensitivity data alone appear to be insufficient to characterize the deformation behaviour. Maximum m-values close to 0.5 observed in the present work are smaller as compared to 0.7 observed by Morgan and Hammond [4] in the same alloy at 830°C, at similar strain rates. However, it may be pointed out that m-values in the present work were obtained from the slopes between adjacent points on bestfit ln σ vs. ln ε' curves, whereas m-values were calculated from slopes between adjacent points on

TABLE I

Temp (°C)	Strain rates (s^{-1})	Max. m	% Elongation
830	6×10^{-5}–3×10^{-3}	0.49	250
850	4×10^{-5}–3×10^{-3}	0.48	542*
855	3×10^{-5}–4×10^{-3}	0.48	634*
865	4×10^{-5}–3×10^{-3}	0.52	410
900	6×10^{-5}–3×10^{-3}	0.54	310
925	6×10^{-5}–3×10^{-3}	0.48	230

*not fractured.

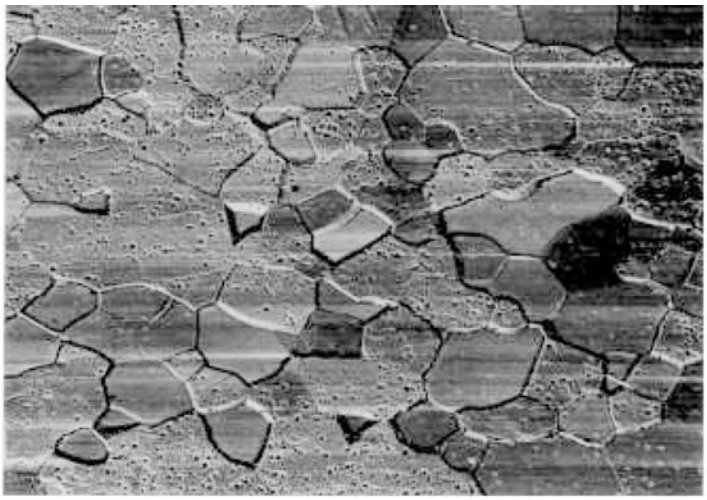

(a) Grip, longitudinal section 100 μm

(b) Gauge length, longitudinal section 100 μm

Figure 5 SEM Micrographs corresponding to Fig. 4.

experimental curves by Morgan and Hammond. Also the strain rate range used by these authors included very low strain rates which were not used in the present investigation. These differences apparently explain the observation of lower m-values than Morgan ad Hammond. Also these authors reported a peak in m-values at 830°C in the temperature range 762–875°C. In the present study maximum m-values varied only between 0.48 and 0.54, the highest value being at 900°C. From these data, it is difficult to establish any relationship between m-values and temperature, but these data nevertheless suggest that the effect of temperature on strain rate sensitivity is very small in this β-titanium alloy, in the temperature range studied.

The ln σ vs. ln ε' curves for the alloy representing up –cycles can be divided into two regions, one at lower strain rates corresponding to high m-values and the other at high strain rates corresponding to low m-values. Therefore stress-strain rate curves may be divided into 'region II' at low and intermediate strain rates and 'region III' at strain rates higher than approximately 1×10^{-3} s^{-1}. The absence of region I may be related to the fact that *very low* cross head speeds corresponding to strain rates below $\sim 2 \times 10^{-5}$ s^{-1} were not used. High temperature deformation properties of Ti-3Al-8V-6Cr-4Mo-4Zr alloy were also studied by Morgan [6] who reported that region I was observed in cases where such low strain rate data were included. Otherwise, only region II and III were generally observed otherwise, particularly at high temperatures. The absence of region I was also reported by Griffiths and Hammond [1] in the case of three commercial metastable β titanium alloys in the range 770–900°C.

Microstructures of the specimen tested at 855°C to an elongation of 634% and a total true strain of 1.99 are shown in Figs 4a and 4b. Upon comparison of microstructure of undeformed (grip) region with that of deformed (gauge length) region, it may be seen that an equiaxed β-grain structure has changed into one with curved and cusped grain boundaries. In addition, subgrains have also been formed. Corresponding scanning electron micrographs are also given in Figs 5a and 5b, where microstructural features associated with the deformation are even more clear. These micrographs show that after this maximum extension of 634%, there is no significant change in average grain size in the alloy.

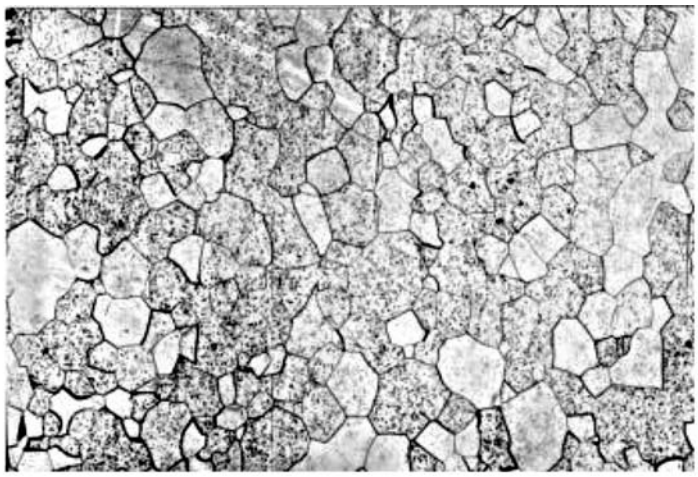

Figure 6 Post test microstructure of Ti-3Al – 8V- 6Cr-4Mo-4Zr specimen deformed at 925°C, corresponding to a true strain of 1.19.

Although grain boundaries are curved and cusped, no grain elongation is observed after the deformation. In addition, grains may also be seen in the process of 'pinching off' as indicated by arrows in Figs 4b and 5b. Similar microstructural features associated with high temperature deformation were reported by Griffiths and Hammond [1] for three metastable β titanium alloys, and by Morgan and Hammond [4] for the alloys Ti-10V-2Fe-3Al and Ti-3Al-8V-6Cr-4Mo-4Zr. In addition to deformation of the grains with sub-grain formation, elongation of grains was also reported by these workers, but it was not very obvious in Ti-3Al-8V-6Cr-4Mo-4Zr. An additional microstructural feature namely strain enhanced grain growth, was reported by Morgan [6] in Ti-3Al-8V-6Cr-4Mo-4Zr at 857 and 875°C, whereas no such effect was seen in this alloy in the present work even at the highest test temperature of 925°C, as shown in Figs. 6a,b, 7a and b, corresponding to a total true strain of 1.19. The absence of strain induced grain growth shows that the strain rate cycling method using a small strain rate range i.e $5 \times 10^{-5}s^{-1}$–$3 \times 10^{-3}s^{-1}$ and excluding low strain rates successfully minimizes the grain growth effects which are generally expected to occur at lower strain rates and higher temperatures. It appears from these results that superplasticity in this alloy arises as a result of deformation by a suitable strain rate cycling method i.e. deformation at a high strain rate initially to develop a subgrain network and repeated cycling at strain rates corresponding to both regions II and III to maintain the subgrain network.

Activation energy values for this alloy were calculated from the slopes of $\ln(\sigma^n / TG^{n-1})$ vs. $1/T$ and $\ln(\varepsilon' TG^{n-1})$ vs. 1/T plots, at constant strain rates and constant stresses by a method given in a previous work of the same authors [7]. Flow stress and strain rate values at different temperatures were taken from (i) first increasing strain rate cycles and (ii) second increasing strain rate cycles. It was considered appropriate to determine the effect of temperature on $\ln \sigma$ - $\ln \varepsilon'$ plots using data from first increasing strain rate cycles because with the increasing deformation (during subsequent cycles), flow stresses either decrease or increase or remain unchanged depending upon the strain rate cycling method and/or changes in the microstructure as a result of strain at a given temperature making it difficult to assess the effect of temperature on $\ln \sigma$ - $\ln \varepsilon'$ plots. However activation energy values were also calculated from the $\ln \sigma$ - $\ln \varepsilon'$ data obtained from second increasing strain

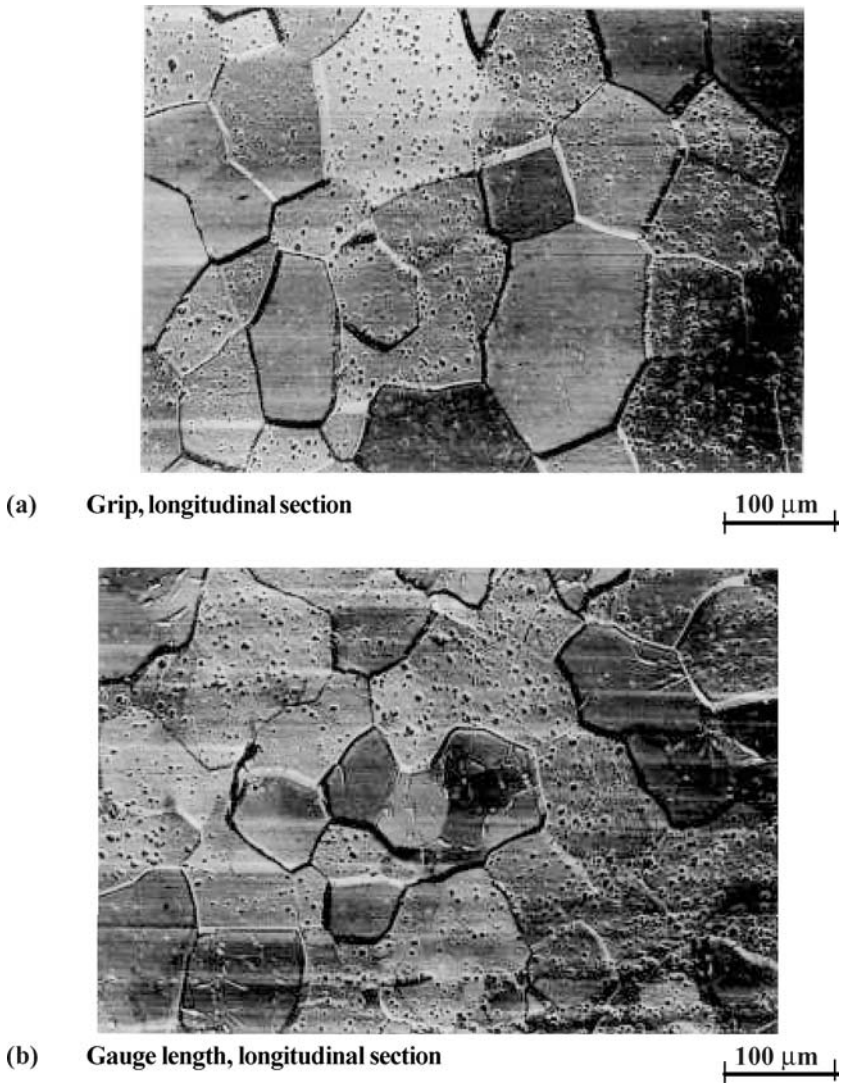

Figure 7 SEM Micrographs corresponding to Fig. 6.

rate cycles. Fig. 8 gives ln (σ^n /TG^{n-1}) vs. $1/T$ plot (at constant $\varepsilon' = 3 \times 10^{-3}$ s^{-1} and Fig. 9 shows ln (ε' TG^{n-1}) vs. $1/T$ plot (at constant $\sigma = 35$ MPa) for the alloy using data from first up cycles. Least squares fit method was used to draw a straight line through the data points. Shear modulus (G) values used in the calculations were taken from a previous work [6]. Stress sensitivity index (n) values for the alloy are given in Table V at different strain rates and stresses. Activation energy values that were calculated using data from first up cycles are given in Table II at constant strain rates, and in Table III at constant stresses, corresponding to regions II and III.

Table II shows that activation energy values calculated for region II and III and not very different. Also it can be seen from Table III that the activation energy values for region II at constant stresses are close to those calculated at constant strain rates. Also, these are in reasonable agreement with the lower of the two activation energy values proposed to describe lattice self-diffusion in β titanium i.e. 129.2 kJ/mole but higher that that expected for grain boundary diffusion. The value calculated for the alloy (for region III) i.e. 128.11 kJ/mole is higher than that found by Morgan [6] for the same alloy (≈78.00 kJ/mole), in the temperature range 762 to 875°C compared to the present work. Activation energy values found by Morgan for Ti-3Al-8V-6Cr-4Mo-4Zr for region II (≈90.00 kJ/mole), taking into account a threshold stress as well can also be seen to be smaller than those obtained in the present work (≈121.23 kJ/mole and 101.15 kJ/mole), However, it is important to point out that the variation of

TABLE II Activation energy values /kJ mole $^{-1}$ (at constant strain rates)

Using ln(σ^n/TG^{n-1}) vs. 1/T plots	Region
128.11	III
121.23	II
101.15	II

TABLE III Activation energy values /kJ mole $^{-1}$ (at constant stress)

ln(ε' TG $^{n-1}$) vs. 1/T	Region
122.28	II/III
103.49	II
118.54	II

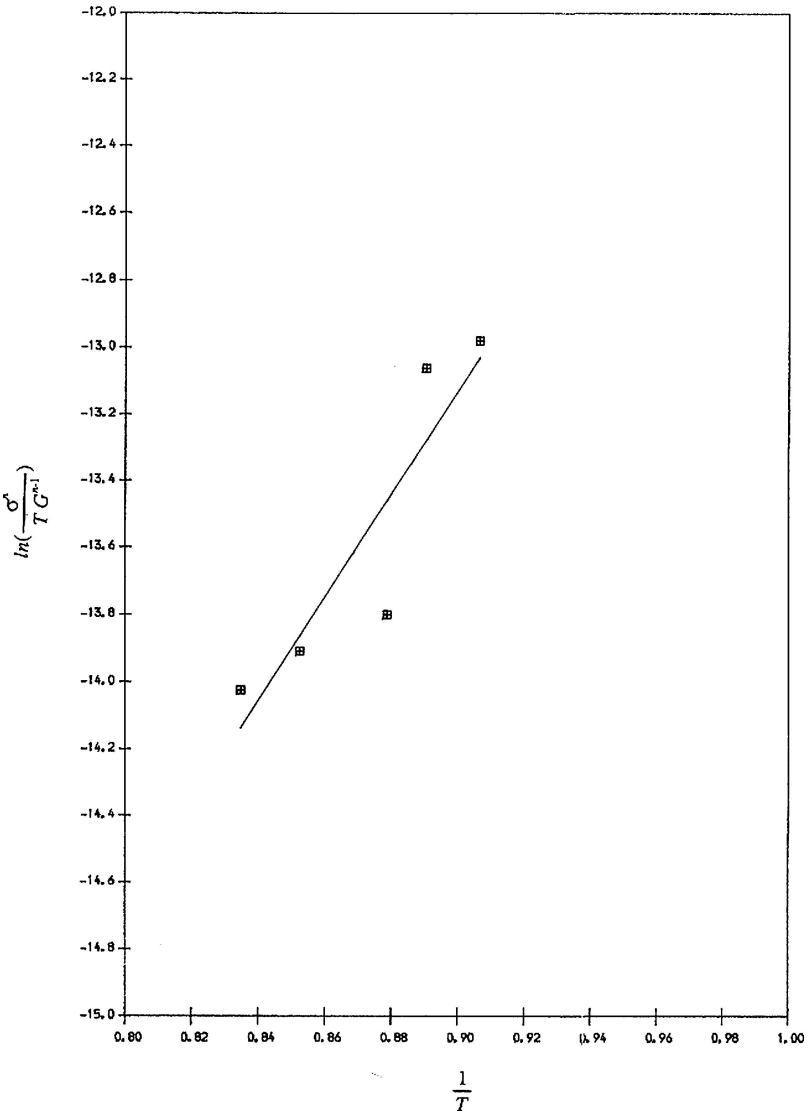

Figure 8 An example of Arrhenius type plot used to calculate the activation energy values for Ti-3A1–8V–6Cr-4Mo-4Zr alloy by constant strain rate method.

shear modulus G with temperature (Table IV) was not taken into account and the variation of stress sensitivity index n was taken as equal to unity by Morgan [6], to calculate activation energy values for region II, whereas in the present work the variation of G with temperature has been taken into account and the experimentally observed values of n were used in the calculations.

As the activation energy values for this alloy found in the present work is in reasonable agreement with the lower of the two values proposed to describe lattice self diffusion in the β-phase, it is considered here that lattice diffusion in the β-phase is the rate controlling mechanism in both regions II and III.

TABLE IV Shear modulus G values

Temp.°C	800	830	845	850	865	900	920	925
Shear modulus G $\times 10^4$ (MPa)	1.26	1.19	1.15	1.14	1.09	1.01	0.955	0.943

Reference [6].

TABLE V Stress sensitivity index (n)

Strain rate/stress	1st up cycle	2nd up cycle
$\varepsilon' = 2 \times 10^{-3}$ s^{-1}	3.07	3.07
$\varepsilon' = 4 \times 10^{-4}$ s^{-1}	–	2.75
$\varepsilon' = 5 \times 10^{-4}$ s^{-1}	2.45	–
$\varepsilon' = 9 \times 10^{-5}$ s^{-1}	1.97	–
$\varepsilon' = 1 \times 10^{-4}$ s^{-1}	–	2.33
$\sigma = 50$ MPa	2.90	–
$\sigma = 40$ MPa	–	3.00
$\sigma = 35$ MPa	2.51	–
$\sigma = 30$ MPa	–	2.79
$\sigma = 22$ MPa	–	2.52
$\sigma = 20$ MPa	2.19	–

4. Conclusions

Following conclusion may be drawn from above work.

(i) Ti-3 Al-8V-6Cr-4Mo-4Zr alloy is superplastic in a narrow temperature range 850–865°C (above the β-transition temperature).

(ii) Maximum elongation of 634% was obtained at 855°C.

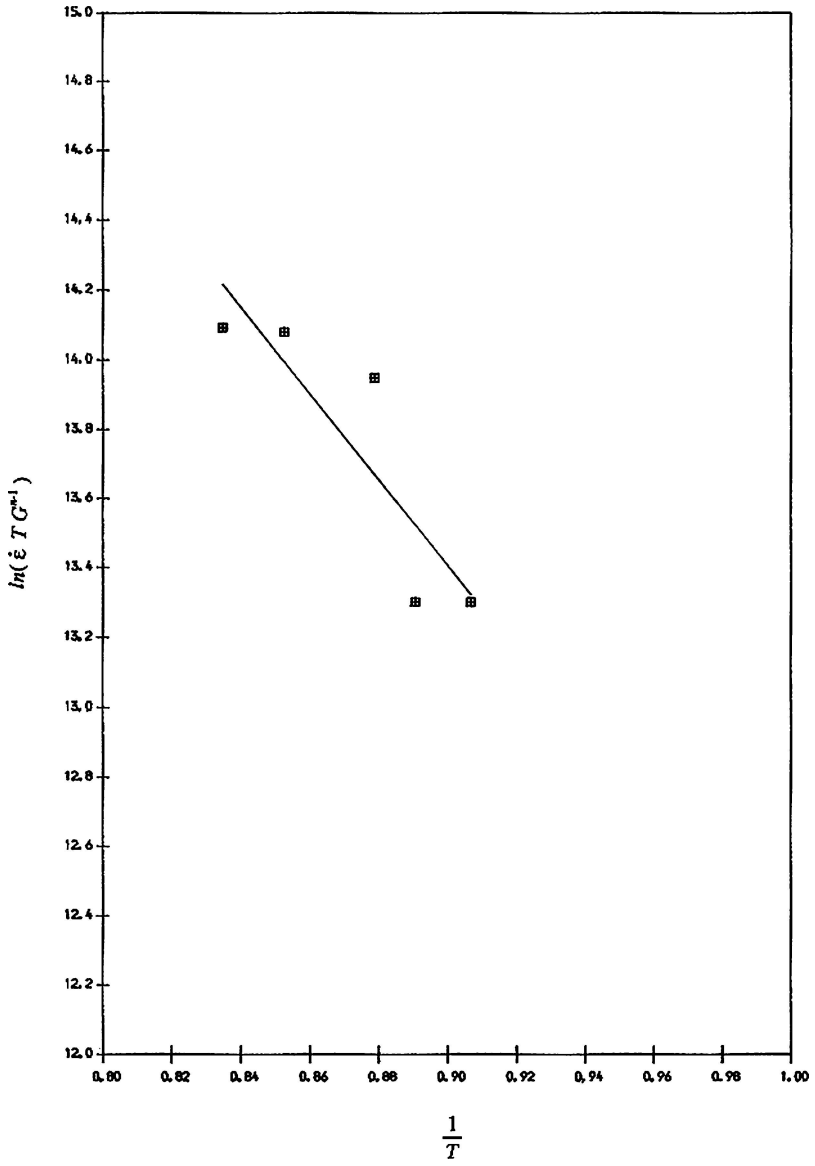

Figure 9 An example of Arrhenius type plot used to calculate the activation energy values for Ti-3A1–8V–6Cr-4Mo-4Zr alloy by constant strees rate method.

(iii) Maximum strain rate sensitivity values approaching 0.5 were observed at lower strain rates.

(iv) The superplastic behariour in this alloy arises as a result of deformation at strain rates which correspond to both regions II and III of ln σ vs. ln ε' plots. Subgrains formed at high strain rates (region III) deform by diffusional creep at lower strain rates resulting in high strain rate sensitivity values at these strain rates.

(v) The superplastic behaviour in this alloy is also attributed to the use of a short strain rate range excluding very low strain rates which minimized the grain growth.

(vi) The activation energy values for regions II and III are close to the lower of the two activation energy proposed to describe self diffusion in β-phase suggesting that the rate controlling mechanism during high temperature of the alloy was that for lattice diffusion.

(vii) This β titanium alloy has high strain rate sensitivity values, large elongations and a constant microstructure which are characteristics of conventional two phase superplastic alloys. This alloy, therefore, could be considered a potential candidate for industrial superplastic forming processes.

Acknowledgement

The author wishes to thank Ministry of Science and Technology, Govt. of Pakistan for the financial support which made this work possible.

References

1. P. GRIFFITHS and C. HAMMOND, *Acta Metall.* **20** (1972) 935.
2. *Idem.*, *Ibid.* **7** (1973) 793.
3. C. H. HAMILTION, S. P. AGRAWAL, N. E. PATON, J. C. CHESNUTT and E. D. WEISERT, Rep. J/0442A/Cb, undated (Rockwell International Science Centre).
4. G. C. MORGAN and C. HAMMOND, *Mat. Sci. Eng.* **86** (1987) 159.
5. A. SALAM and C. HAMMOND, *Proc. Conf. France* (1988) 1355.
6. G. C. MORGAN, Ph. D. Thesis, University of Leeds, U.K. (1981).
7. A. SALAM and C. HAMMOND, *J. Mat. Sci. Lett.* **19** (2000) 2155.

Received 10 March 2004
and accepted 16 February 2005